Measurements of the angle α at B factories

G. Vasseur * †
CEA, Irfu, SPP, Centre de Saclay, F-91191 Gif sur Yvette, France

The determinations of the angle α of the unitarity triangle at the B factories are reviewed with some emphasis on the updated measurement in the $B \to \rho\rho$ decay modes. When combining the results obtained in the $B \to \pi\pi$, $B \to \rho\pi$, and $B \to \rho\rho$ modes by both the *BABAR* and Belle experiments, a precise measurement of α is obtained: $\alpha = (89.0^{+4.4}_{-4.2})^\circ$.

I. INTRODUCTION

A. The angle α

CP violation in the quark sector is explained in the standard model (SM) through the complex Cabibbo-Kobayashi-Maskawa (CKM) quark-mixing matrix [1]. A relation due to the unitarity of the CKM matrix, $V_{ud}V_{ub}^* + V_{cd}V_{cb}^* + V_{td}V_{tb}^* = 0$, is represented graphically in the complex plane as the unitarity triangle, shown in Figure 1.

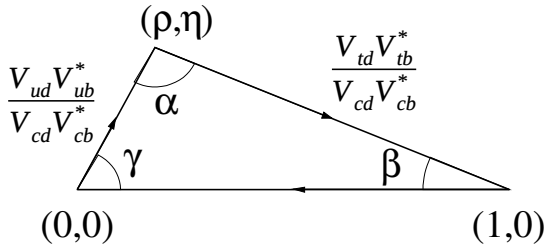

FIG. 1: The unitariry triangle and its three angles α, β, and γ.

The main goal of the *BABAR* and Belle experiments is to test the SM explanation of CP violation in over-constraining the unitarity triangle, by measuring its sides and its three angles α, β, and γ (also called ϕ_2, ϕ_1, and ϕ_3 respectively). The angle $\alpha = \arg(-\frac{V_{td}V_{tb}^*}{V_{ud}V_{ub}^*})$ brings into play the two elements of the CKM matrix which are non real at lowest order: V_{td}, involved in $B^0\bar{B}^0$ mixing, whose phase is $-\beta$, and V_{ub}, involved in decays proceeding via a b to u transtion, whose phase is $-\gamma$. So $\alpha = \pi - \beta - \gamma$ can be measured from CP violating asymmetries in the interference between mixing and decay in charmless decays of the neutral B mesons, such as $B^0 \to \pi^+\pi^-$, $B^0 \to \rho^+\rho^-$, $B^0 \to \pi^+\pi^-\pi^0$, and $B^0 \to a_1^\pm\pi^\mp$.

*e-mail: georges.vasseur@cea.fr
†Presented at the 22nd workshop on Weak Interactions and Neutrinos, Perugia, Italy, September 14-19, 2009.

B. Analyses overview

The *BABAR* and Belle detectors [2] at the PEP-II and KEK-B e^+e^- colliders respectively are very similar in design and in performance. Both experiments have now in hand their final data sample on the $\Upsilon(4S)$ resonance, about 780×10^6 $B\bar{B}$ pairs for Belle and 470×10^6 $B\bar{B}$ pairs for *BABAR*.

The decay modes relevant to measure α have only pions in the final state. Charged pions are reconstructed in tracking chambers and identified mainly with Cherenkov detectors. Neutral pions decay into two photons reconstructed using the electromagnetic calorimeter.

The largest background consists of $q\bar{q}$ ($q = u, d, s, c$) continuum events. Event shape variables are used to separate the jet-like continuum events from the more spherical $B\bar{B}$ events. The beam-energy constrained B-meson mass $m_B = \sqrt{E^2_{\rm beam} - p^2_B}$ and the energy difference $\Delta E = E_B - E_{\rm beam}$ are powerful kinematic discriminating variables, peaking respectively for the signal at the B-meson mass and zero. $E_{\rm beam}$ is the beam energy. E_B and p_B are the energy and momentum of the reconstructed candidate, all evaluated in the $\Upsilon(4S)$ rest frame. The discriminating variables are used as inputs to multi-variable maximum likelihood fits in most analyses presented in this review.

C. Time-dependent CP asymmetry

At the $\Upsilon(4S)$ resonance, $B\bar{B}$ pairs are produced in a coherent state. The CP asymmetry is measured as a function of the difference Δt between the decay times of the two B mesons, which in an energy-asymmetric machine is obtained from the measured distance Δz along the beam axis between the two vertices according to $\Delta t = \Delta z/\beta\gamma c$. Here c is the speed of light and $\beta\gamma$, equal to 0.56 in *BABAR* and 0.425 in Belle, is the average Lorentz boost of the $\Upsilon(4S)$.

One of the B mesons is fully reconstructed into the B decay of interest ($\pi\pi$, $\rho\pi$, $\rho\rho$, or $a_1\pi$), while the other B meson is used to tag its flavor at production time. Tagging combines different techniques including the use of semileptonic decays and secondary kaons.

A B^0 meson can decay into a given CP eigenstate f either directly or after having oscillated to a $\bar{B}^0$

meson which decays to f. The amplitudes associated to these two processes are respectively A_f and $\frac{q}{p}\bar{A}_f$ where $\frac{q}{p} \sim e^{-2i\beta}$ accounts for $B^0\bar{B}^0$ mixing. The resulting CP violation asymmetry as a function of the proper time difference Δt can be expressed as:

$$\begin{aligned} a(\Delta t) &= \frac{\Gamma_{\bar{B}^0\to f}(\Delta t) - \Gamma_{B^0\to f}(\Delta t)}{\Gamma_{\bar{B}^0\to f}(\Delta t) + \Gamma_{B^0\to f}(\Delta t)} \\ &= S\sin(\Delta m\Delta t) - C\cos(\Delta m\Delta t) \end{aligned} \quad (1)$$

where Δm is the mass difference between the two neutral B mass eigenstates. The coefficients $C = \frac{1-|\lambda_f|^2}{1+|\lambda_f|^2}$ and $S = \frac{2\Im(\lambda_f)}{1+|\lambda_f|^2}$ are functions of the ratio of the amplitudes with and without mixing $\lambda_f = \frac{q}{p}\frac{\bar{A}_f}{A_f}$. C (or $\mathcal{A} = -C$) measures direct CP violation while S measures CP violation in the interference between decay and mixing.

In the simple case of a charmless B^0 decay involving only the b to u tree diagram amplitude, with weak phase γ, we have $\lambda_f = e^{-2i\beta}e^{-2i\gamma} = e^{2i\alpha}$, resulting in $C = 0$ and $S = \sin 2\alpha$. A time-dependent analysis of the CP asymmetry in this mode would give a direct measurement of α. However other diagrams are involved in charmless decays and in particular the one loop gluonic penguin diagrams. As the dominant gluonic penguin diagram does not carry the same weak phase as the tree diagram, the extraction of α becomes more complex. C is no longer equal to 0 and $S = \sqrt{1-C^2}\sin 2\alpha_{\rm eff}$ does not any more measure α but an effective value $\alpha_{\rm eff}$.

Additional information is needed to extract α. The usual method are based on SU(2) symmetry, SU(3) symmetry, or Dalitz plot information.

D. The isospin analysis

The isospin analysis [3], based on SU(2) symmetry, allows the extraction of the true value of α by determining the difference $\alpha - \alpha_{\rm eff}$. It can be applied both to the $B \to \pi\pi$ and $B \to \rho\rho$ modes with the advantage in $B \to \rho\rho$ that the ratio of penguin over tree amplitude is smaller. It relates the amplitudes of all the $B \to hh$ ($h = \pi$ or ρ) decay modes: $A^{+-} = A(B^0 \to h^+h^-)$, $A^{+0} = A(B^+ \to h^+h^0)$, $A^{00} = A(B^0 \to h^0h^0)$, $\widetilde{A}^{+-} = A(\bar{B}^0 \to h^+h^-)$, $\widetilde{A}^{-0} = A(B^- \to h^-h^0)$, and $\widetilde{A}^{00} = A(\bar{B}^0 \to h^0h^0)$. Neglecting electroweak penguin diagrams and other SU(2)-breaking effects and using the fact that the amplitude of the pure tree $B^+ \to h^+h^0$ mode is equal to the one of its charge conjugate process, we obtain the isospin relations:

$$\frac{A^{+-}}{\sqrt{2}} + A^{00} = A^{+0} = \widetilde{A}^{-0} = \frac{\widetilde{A}^{+-}}{\sqrt{2}} + \widetilde{A}^{00} \quad (2)$$

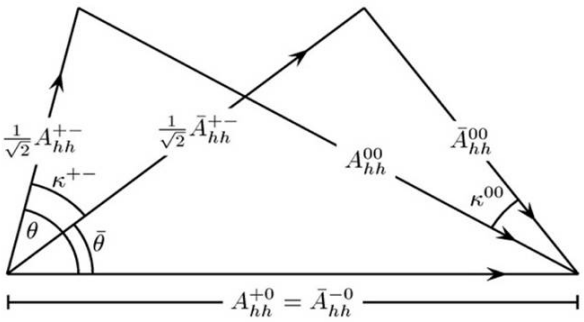

FIG. 2: Graphical representation of the isospin relations.

These relations are represented graphically as two triangles with a common base, shown in Figure 2. Measuring the length of the sides of the two triangles, related to the branching ratios of the various modes, constrains the angle $\kappa^{+-} = 2(\alpha - \alpha_{\rm eff})$. As both triangles have two possible orientations, up and down, the isospin method has a four-fold ambiguity, which comes in addition to the two-fold ambiguity related to the fact that only the sine of $2\alpha_{\rm eff}$ is measured in the time-dependent analysis of $B^0 \to h^+h^-$. The four-fold ambiguity can be resolved by measuring the angle κ^{00} through a time-dependent analysis of the color suppressed $B^0 \to h^0h^0$ decay mode.

II. $B \to \pi\pi$ DECAYS

The time-dependent CP asymmetry of the $B^0 \to \pi^+\pi^-$ decays has been studied by Belle with 1464 ± 65 signal events [4] and by *BABAR* on the final data sample with 1394 ± 54 signal events [5]. The measurements of $S_{\pi^+\pi^-}$ and $C_{\pi^+\pi^-}$ are summarized in Table I. Both experiments have observed CP violation in the interference between decay and mixing in the $B^0 \to \pi^+\pi^-$ decays as the $S_{\pi^+\pi^-}$ parameter is found different from 0 with a significance of more than 5 σ with a good agreement between the two experiments. In addition Belle sees a 5.5 σ effect also for the direct CP violation parameter $C_{\pi^+\pi^-}$, which is somewhat different from the *BABAR* result, at the level of 2 σ, but not inconsistent with it.

All the $B \to \pi\pi$ modes, which are needed to perform the isospin analysis, have been measured by *BABAR* [5–7] and Belle [8–10]. The results and the world averages [11] for the branching ratios, as well as the time-integrated asymmetries are given in Table I. The branching ratio of $B^0 \to \pi^0\pi^0$, whose tree diagram is color supressed, is relatively large, about 30% of that of $B^0 \to \pi^+\pi^-$, thus indicating a large penguin contamination in $B \to \pi\pi$. The charge asymmetry in $B^+ \to \pi^+\pi^0$ is compatible with 0 as expected.

Using the six observables (the branching fraction of the three $B \to \pi\pi$ modes, $S_{\pi^+\pi^-}$, $C_{\pi^+\pi^-}$, and $C_{\pi^0\pi^0}$) an isospin analysis is performed to determine the six

	BABAR			Belle			World average
	Result	$N_{B\bar{B}}$	Ref.	Result	$N_{B\bar{B}}$	Ref.	
$S_{\pi^+\pi^-}$	$-0.68 \pm 0.10 \pm 0.03$	467M	[5]	$-0.61 \pm 0.10 \pm 0.04$	535M	[4]	-0.65 ± 0.07
$C_{\pi^+\pi^-}$	$-0.25 \pm 0.08 \pm 0.02$	467M	[5]	$-0.55 \pm 0.08 \pm 0.05$	535M	[4]	-0.38 ± 0.06
$C_{\pi^0\pi^0}$	$-0.43 \pm 0.26 \pm 0.05$	467M	[5]	$-0.44\,^{+0.62\ +0.06}_{-0.73\ -0.04}$	535M	[8]	-0.43 ± 0.25
$\mathcal{A}_{\pi^+\pi^0}$	$0.03 \pm 0.08 \pm 0.01$	383M	[6]	$0.07 \pm 0.06 \pm 0.01$	535M	[9]	0.06 ± 0.05
$\mathcal{B}(B^0 \to \pi^+\pi^-)$	$(5.5 \pm 0.4 \pm 0.3)10^{-6}$	227M	[7]	$(5.1 \pm 0.2 \pm 0.2)10^{-6}$	449M	[10]	$(5.16 \pm 0.22)10^{-6}$
$\mathcal{B}(B^+ \to \pi^+\pi^0)$	$(5.0 \pm 0.5 \pm 0.3)10^{-6}$	383M	[6]	$(6.5 \pm 0.4 \pm 0.5)10^{-6}$	449M	[10]	$(5.6 \pm 0.4)10^{-6}$
$\mathcal{B}(B^0 \to \pi^0\pi^0)$	$(1.8 \pm 0.2 \pm 0.1)10^{-6}$	467M	[5]	$(1.1 \pm 0.3 \pm 0.1)10^{-6}$	535M	[8]	$(1.55 \pm 0.19)10^{-6}$

TABLE I: : Measurements of CP parameters and branching fractions in the $B \to \pi\pi$ modes. For each result the statistics used for the analysis and the reference are given.

unknown parameters and in particular α. For each value of α, the minimum χ^2 in the fit of the isospin triangles to the measured observables is converted to a frequentist confidence level (CL), shown in Figure 3. The already mentionned discrete ambiguities in the determination of α give several peaks which can be seen on the plot. The range of values between 11° and 79° is excluded by Belle at 95% CL and the one between 23° and 67° is excluded by *BABAR* at 90% CL.

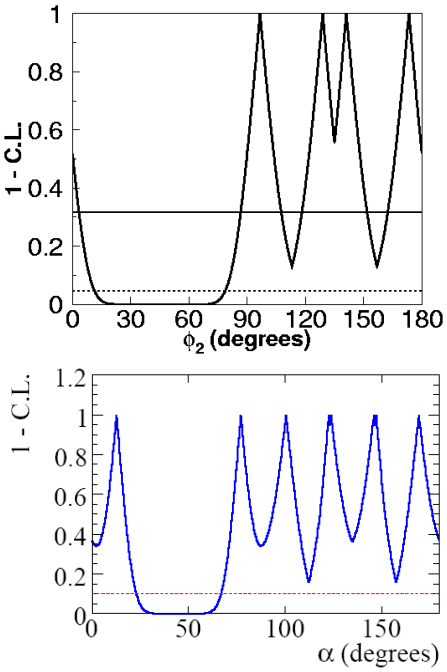

FIG. 3: Constraint on α from the isospin analysis in the $B \to \pi\pi$ modes expressed as 1-CL from (top) Belle and (bottom) *BABAR*. (Top) the horizontal solid and dashed lines correspond to 68% and 95% CL and (bottom) the dashed line to 90% CL.

III. $B \to \rho\rho$ DECAYS

$B \to \rho\rho$ analyses are experimentally more challenging than the $B \to \pi\pi$ analyses as the final states consist of four pions, including two π^0 for the $\rho^+\rho^-$ mode. The wide ρ resonance also results in more background. Finally these vector-vector modes have in principle three partial waves with mixed CP eigenstates. Fortunately the $B^0 \to \rho^+\rho^-$ mode is nearly 100% longitudinally polarized and consequently it is an almost pure CP-even state. Besides the $B^0 \to \rho^+\rho^-$ branching ratio is about five times larger than the one of $B^0 \to \pi^+\pi^-$, and the ratio of penguin over tree amplitude is smaller. Thus this mode turns out to be better for constraining α.

A similar time-dependent analysis to that for the $B^0 \to \pi^+\pi^-$ mode is performed for $B^0 \to \rho^+\rho^-$, with the reconstructed masses of the two ρ mesons as well as their helicity angles $\theta_{1,2}$ as additional observables, and the fraction f_L of longitudinal polarization as an additional parameter. The angular dependence of the decay rate is: $\frac{d\Gamma}{d\theta_1 d\theta_2} \propto \frac{1-f_L}{4} \sin^2\theta_1 \sin^2\theta_2 + f_L \cos^2\theta_1 \cos^2\theta_2$. Using respectively 576 ± 53 signal events [12] and 729 ± 60 signal events [13], the Belle and *BABAR* experiments have measured the CP parameters $S_{\rho^+\rho^-}$ and $C_{\rho^+\rho^-}$, given in Table II. The agreement between the two experiments is good.

The isospin analysis of the longitudinal component of the $B \to \rho\rho$ modes is then performed. The other ingredients for this analysis, the branching fraction, the fraction of longitudinal polarization and the remaining CP parameters, for all the $B \to \rho\rho$ decay modes have been measured by *BABAR* [13–15] and by Belle [16–18], as summarized in Table II.

The small value of the $B^0 \to \rho^0\rho^0$ branching ratio compared to the one of the other channels, less than 5%, shows that the penguin contribution is small in the $B \to \rho\rho$ modes. The two experiments obtain somewhat different results for the $B^0 \to \rho^0\rho^0$ mode, though not inconsistent. While Belle does not see any significant signal [18], *BABAR* finds evidence for this decay [14] based on 99 ± 35 signal events with a signifi-

	BABAR			Belle			World average
	Result	$N_{B\bar{B}}$	Ref.	Result	$N_{B\bar{B}}$	Ref.	
$S_{\rho^+\rho^-}$	$-0.17 \pm 0.20 \pm 0.06$	384M	[13]	$0.19 \pm 0.30 \pm 0.08$	535M	[12]	-0.05 ± 0.17
$C_{\rho^+\rho^-}$	$0.01 \pm 0.15 \pm 0.06$	384M	[13]	$-0.16 \pm 0.21 \pm 0.08$	535M	[12]	-0.06 ± 0.13
$S_{\rho^0\rho^0}$	$0.3 \pm 0.7 \pm 0.2$	465M	[14]	-			0.3 ± 0.9
$C_{\rho^0\rho^0}$	$0.2 \pm 0.8 \pm 0.3$	465M	[14]	-			0.2 ± 0.9
$\mathcal{A}_{\rho^+\rho^0}$	$-0.05 \pm 0.06 \pm 0.01$	465M	[15]	$0.00 \pm 0.22 \pm 0.03$	85M	[17]	-0.05 ± 0.05
$\mathcal{B}(B^0 \to \rho^+\rho^-)$	$(25 \pm 2 \pm 4)10^{-6}$	384M	[13]	$(23 \pm 4^{+2}_{-3})10^{-6}$	275M	[16]	$(24 \pm 3)10^{-6}$
$\mathcal{B}(B^+ \to \rho^+\rho^0)$	$(23.7 \pm 1.4 \pm 1.4)10^{-6}$	465M	[15]	$(32 \pm 7^{+4}_{-7})10^{-6}$	85M	[17]	$(24 \pm 2)10^{-6}$
$\mathcal{B}(B^0 \to \rho^0\rho^0)$	$(0.9 \pm 0.3 \pm 0.1)10^{-6}$	465M	[14]	$(0.4 \pm 0.4^{+0.2}_{-0.3})10^{-6}$	657M	[18]	$(0.7 \pm 0.3)10^{-6}$
$f_L^{\rho^+\rho^-}$	$0.99 \pm 0.02^{+0.03}_{-0.01}$	384M	[13]	$0.94^{+0.03}_{-0.04} \pm 0.03$	275M	[16]	0.98 ± 0.02
$f_L^{\rho^+\rho^0}$	$0.95 \pm 0.02 \pm 0.01$	465M	[15]	$0.95 \pm 0.11 \pm 0.02$	85M	[17]	0.95 ± 0.02
$f_L^{\rho^0\rho^0}$	$0.75^{+0.11}_{-0.14} \pm 0.05$	465M	[14]	-			0.75 ± 0.15

TABLE II: Measurements of CP parameters, branching fractions, and fractions of longitudinal polarization in the $B \to \rho\rho$ modes. For each result the statistics used for the analysis and the reference are given.

cance of 3.1 σ taking into account the systematics. As the decay vertex of the $\rho^0\rho^0$ final state can be reconstructed in contrast to $\pi^0\pi^0$, a time-dependent analysis is possible. *BABAR* has demonstrated the feasibility of such an analysis and given a first measurement of $C_{\rho^0\rho^0}$ and $S_{\rho^0\rho^0}$.

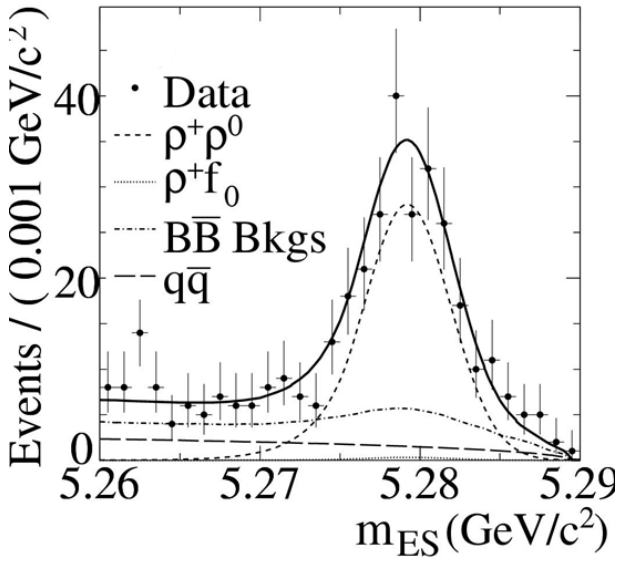

FIG. 4: Distribution of m_B in the recent $B^+ \to \rho^+\rho^0$ analysis from *BABAR*. The points are the data. The solid curve is the projection of the fit onto m_B. The various components are shown: $\rho^+\rho^0$ signal (dashed curve), $\rho^+ f_0$ (dotted curve), $B\bar{B}$ backgrounds (dot-dashed curve), and continuum background (large dashed curve).

The last input to the isospin analysis is the branching ratio of $B^+ \to \rho^+\rho^0$. The measurement from Belle, which was the first observation of this decay [17], was performed on a now small data sample. *BABAR* has published recently a new result [15] based on the final data sample. The $B^+ \to \rho^+\rho^0$ signal of 1122 ± 63 events, illustrated in Figure 4, leads to a branching fraction about 2 σ higher than the previous result from *BABAR* with half the statistics. The direct CP asymmetry is compatible with 0 as expected for this mode, dominated by a single amplitude.

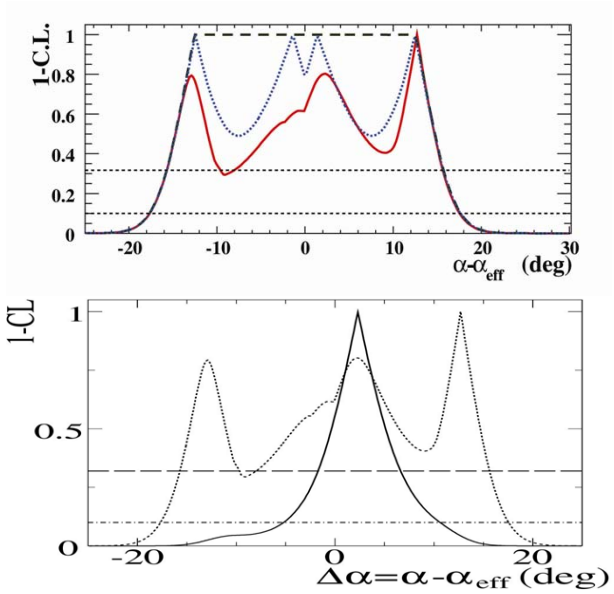

FIG. 5: Constraint on $\alpha - \alpha_{\rm eff}$ obtained by *BABAR* from the isospin analysis in the $B \to \rho\rho$ modes expressed as 1-CL. The top plot shows the impact of the time-dependent analysis in $B^0 \to \rho^0\rho^0$: constraint on $\alpha - \alpha_{\rm eff}$ including the measurements of $C_{\rho^0\rho^0}$ and $S_{\rho^0\rho^0}$ (solid curve), the measurement of $C_{\rho^0\rho^0}$ only (dotted curve) and none of them (dashed curve). The bottom plot shows the constraint on $\alpha - \alpha_{\rm eff}$ with the new result on $B^+ \to \rho^+\rho^0$ (solid curve) compared to the one with the previous result (dotted curve). On both plots, the horizontal dashed lines correspond to 68% and 90% CL.

The impact of measuring $C_{\rho^0\rho^0}$ and $S_{\rho^0\rho^0}$ for the isospin analysis in $B \to \rho\rho$ is shown on the top plot of Figure 5. Without these two parameters, we have only five observables for six unknown parameters and the isospin analysis gives a plateau of degenerated values for $\alpha - \alpha_{\rm eff}$. Adding $C_{\rho^0\rho^0}$, we have now as many observables as unknown and find the four ambiguities inherent in the isospin analysis. If we also measure $S_{\rho^0\rho^0}$, which gives seven observables for six unknown, the isospin analysis is able to favor one single solution. With the current precision, the discrimination between the four solutions is however limited. The overall constraint at 1 σ level was $|\alpha - \alpha_{\rm eff}| < 16^\circ$ [14] last year. This year the new value for the branching fraction of $B^+ \to \rho^+\rho^0$ from *BABAR* has increased the length of the base of the isospin triangles, flattening them. It results in a better determination of $\alpha - \alpha_{\rm eff}$ and merges the discrete ambiguities, as illustrated in the bottom plot of Figure 5. The new constraint at 1 σ level is $-1.8 < \alpha - \alpha_{\rm eff} < 6.7^\circ$ [15].

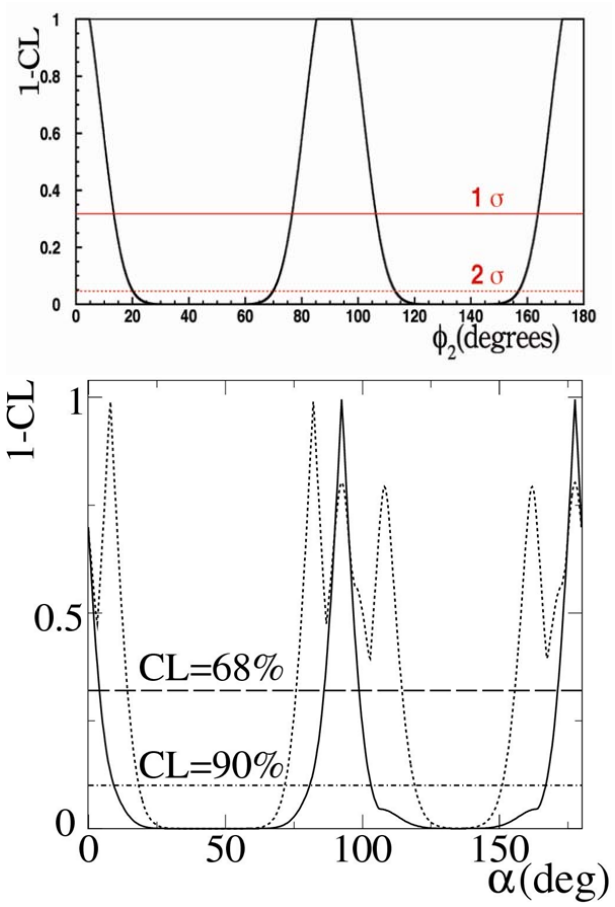

FIG. 6: Constraint on α from the isospin analysis in the $B \to \rho\rho$ modes expressed as 1-CL from (top) Belle and (bottom) *BABAR* with the old result for the branching ratio of $B^+ \to \rho^+\rho^0$ (dotted curve) and the new one (solid curve). The horizontal lines correspond to 68% and (top) 95% or (bottom) 90% CL.

The outcome of the isospin analysis in the $B \to \rho\rho$ modes for the determination of the angle α itself is shown in Figure 6. The top plot from Belle was obtained last year with the value of the branching fraction of $B^0 \to \rho^0\rho^0$ from Belle and the world averages at that time for the other branching fractions. Choosing the solution consistent with the other CKM measurements, this gave a measurement of α of $(92 \pm 15)^\circ$. *BABAR* had a similar measurement last year using the measurements of all the $B \to \rho\rho$ modes from *BABAR*. The new result for the branching fraction of $B^+ \to \rho^+\rho^0$ has now improved a lot the precison on α, as illustrated on the bottom plot of Figure 6. Choosing again the solution consistent with the other CKM measurements, the determination of α from the $B \to \rho\rho$ modes is $(92.4^{+6.0}_{-6.5})^\circ$. A future measurement of this branching fraction by Belle using its large data sample has the potential to improve further our knowledge of α. At this level of precision, SU(2)-breaking effects may become non negligible. A possible way out is to consider other methods to determine α.

An alternative approach to measure α is to use flavor SU(3) symmetry to constrain the penguin contribution in $B^0 \to \rho^+\rho^-$ with the longitudinal component of the pure penguin $B^+ \to K^{*0}\rho^+$ channel [19]. The latter mode has been measured by Belle using 275×10^6 $B\bar{B}$ pairs [20] and by *BABAR* using 232×10^6 $B\bar{B}$ pairs [21] with a good agreement between the two experiments. It gives the following world averages: $\mathcal{B}(B^+ \to K^{*0}\rho^+) = (9.2 \pm 1.5)10^{-6}$ and $f_L^{K^{*0}\rho^+} = 0.48 \pm 0.08$. The method has three unknown parameters: the ratio of penguin over tree amplitudes in $B^0 \to \rho^+\rho^-$, the relative phase between these penguin and tree amplitudes and α. Taking SU(3)-breaking effect into account, it gives a good constraint on α: $83 < \alpha < 106^\circ$ at 1 σ level [13], as illustrated in Figure 7.

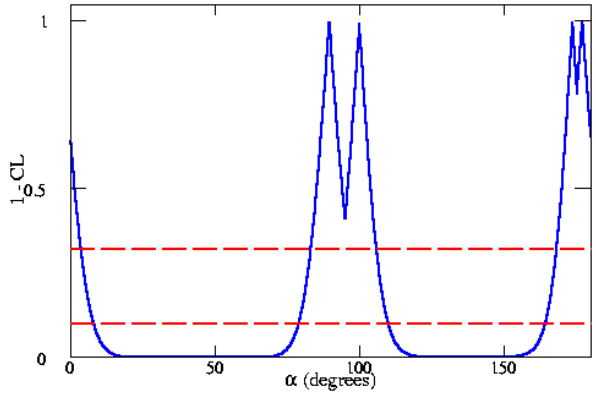

FIG. 7: Constraint on α from the SU(3) analysis of the $B^0 \to \rho^+\rho^-$ and $B^+ \to K^{*0}\rho^+$ modes expressed as 1-CL from *BABAR*. The horizontal dashed lines correspond to 68% and 90% CL.

IV. $B \to \pi\pi\pi$ DECAYS

The $B^0 \to \rho^\pm\pi^\mp$ decay is not a CP eigenstate like $\pi^+\pi^-$ or $\rho^+\rho^-$. An isospin analysis would not constrain sufficiently the five amplitudes of the B decays to $\rho^+\pi^-$, $\rho^-\pi^+$, $\rho^0\pi^0$, $\rho^+\pi^0$, and $\rho^0\pi^+$. A better approach [22] is based on the time-dependent analysis of the $B^0 \to \pi^+\pi^-\pi^0$ decay over the Dalitz plot, using the isospin symmetry as an additional constraint. As this $B \to 3\pi$ decay is dominated by $\rho\pi$ resonances, its amplitude is a function of well-known kinematic functions of the Dalitz variables and of the $B^0 \to \rho\pi$ amplitudes. The time-dependent CP analysis of the $B^0 \to \pi^+\pi^-\pi^0$ decay provides enough constraints to extract α without discrete ambiguities.

The analysis has been performed by *BABAR* using 375×10^6 $B\bar{B}$ pairs [23] and Belle using 449×10^6 $B\bar{B}$ pairs [24] corresponding to 2067 ± 68 and 971 ± 42 signal events respectively. The resulting constraints on α are illustrated in Figure 8: $68 < \alpha < 95°$ for Belle and $74 < \alpha < 132°$ for *BABAR* at 1 σ level.

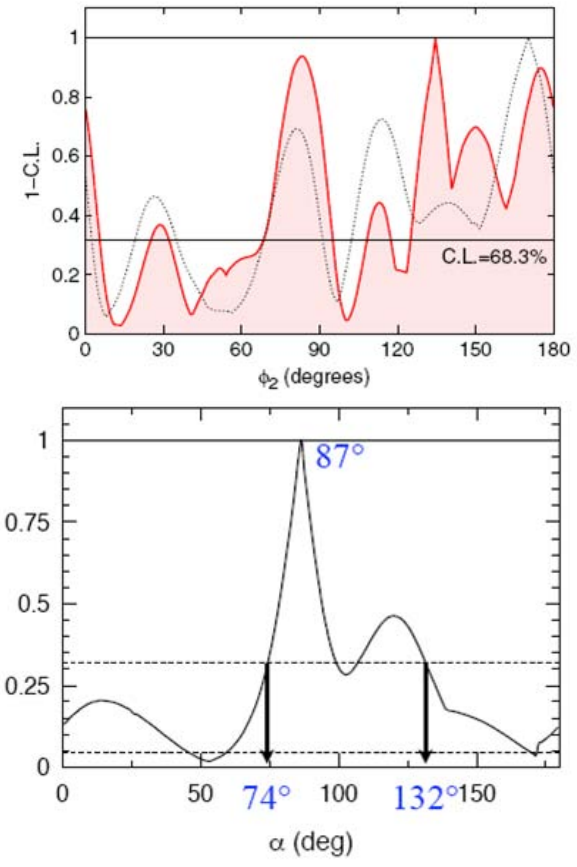

FIG. 8: Constraint on α from the Dalitz analysis in the $B \to \rho\pi$ modes expressed as 1-CL from (top) Belle and (bottom) *BABAR*. On the top plot, the solid (dotted) curve is obtained with (without) the additional isospin constraint. The horizontal lines correspond to 68% and (bottom only) 95% CL.

V. $B \to a_1\pi$ DECAYS

The $B \to a_1\pi$ modes also allow the measurement of α. The $B^0 \to a_1^\pm\pi^\mp$ channel has a high branching fraction, as measured by *BABAR* using 218×10^6 $B\bar{B}$ pairs [25] and by Belle using 535×10^6 $B\bar{B}$ pairs [26]. The two results are in good agreement and give a word average of $(32 \pm 4)10^{-6}$.

The $B^0 \to a_1^\pm\pi^\mp$ mode, like $B^0 \to \rho^\pm\pi^\mp$, is not a CP eigenstate. Using a quasi-two body approach, *BABAR* has performed a time-dependent analysis of this mode based on 384×10^6 $B\bar{B}$ pairs [27]. It is illustrated in Figure 9 by the projection plots onto Δt for B^0 and $\bar{B}^0$ tags, and the asymmetry between B^0 and $\bar{B}^0$ tags. With 608 ± 52 signal events, it leads to the measurement of $\alpha_{\rm eff}^{a_1\pi} = (79 \pm 7)°$.

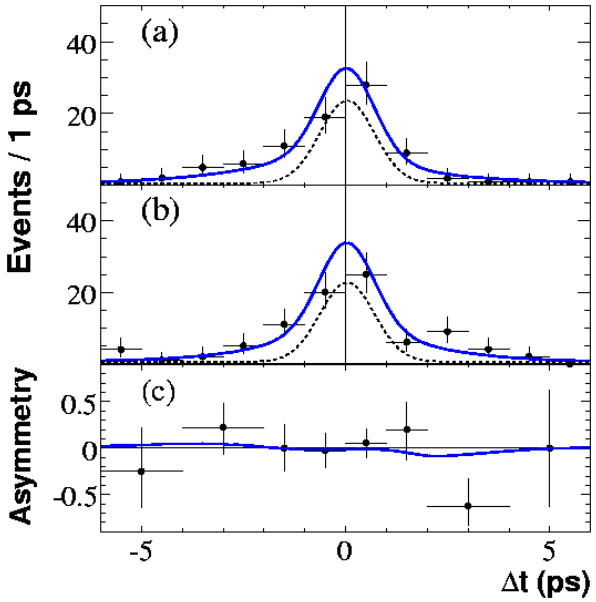

FIG. 9: Projections onto Δt of the $B^0 \to a_1^\pm\pi^\mp$ data from *BABAR* (points) for (a) B^0 and (b)$\bar{B}^0$ tags, showing the fit function (solid line) and the background function (dotted line), and (c) the asymmetry between B^0 and $\bar{B}^0$ tags.

To constrain $\alpha - \alpha_{\rm eff}$, flavor SU(3) symmetry can be used [28]. In addition to $B \to a_1\pi$, the related modes $B \to K_1\pi$ and $B \to a_1K$ have to be measured. Using 383×10^6 $B\bar{B}$ pairs, *BABAR* has studied the $B \to a_1K$ modes [29] and has measured the following branching fractions $\mathcal{B}(B^0 \to a_1^-K^+) = (16 \pm 3 \pm 2)10^{-6}$ and $\mathcal{B}(B^+ \to a_1^+K^0) = (35 \pm 5 \pm 4)10^{-6}$. As for the $B \to K_1\pi$ modes, where K_1 is a mixture of the $K_1(1270)$ and $K_1(1400)$ mesons, they have recently been measured on a data sample of 454×10^6 $B\bar{B}$ pairs by *BABAR* [30]: $\mathcal{B}(B^0 \to K_1^+\pi^-) = (31\,^{+8}_{-7})10^{-6}$ and $\mathcal{B}(B^+ \to K_1^0\pi^+) = (29\,^{+30}_{-17})10^{-6}$. With this last piece of information, an upper bound on $\alpha - \alpha_{\rm eff}$ of 11° at 1 σ can be set. So the measurement of α from the $B \to a_1\pi$ modes is $(79 \pm 7 \pm 11)°$.

VI. SUMMARY

The $B \to \pi\pi$, $B \to \rho\pi$, $B \to \rho\rho$, and $B \to a_1\pi$ decay modes give consistent and complementary measurements of α. The plot from the CKMfitter group [31] in Figure 10 summarizes the constraints on α obtained by combining the results from *BABAR* and Belle, using the isospin analysis in the $B \to \pi\pi$ and $B \to \rho\rho$ modes and the Dalitz plot analysis in the $B \to \rho\pi$ modes. The contribution from the $B \to \pi\pi$ modes is limited by the large penguin pollution. The $B \to \rho\rho$ modes give the most precise single measurement. The $B \to \rho\pi$ modes are important to remove the mirror solution. The current results yield a combined value of $\alpha = (89.0^{+4.4}_{-4.2})^\circ$.

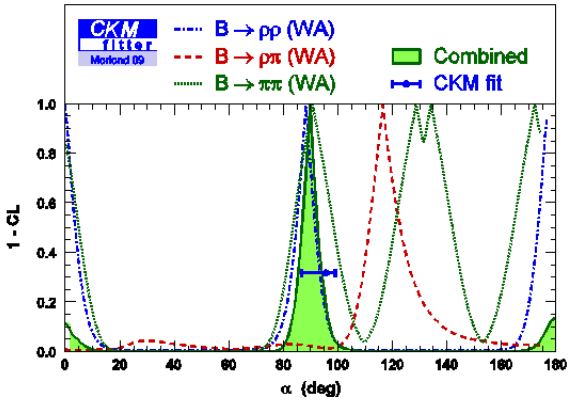

FIG. 10: Combined constraint on α expressed as 1-CL. The individual constraints from the $B \to \pi\pi$, $B \to \rho\rho$, and $B \to \rho\pi$ modes (combining *BABAR* and Belle results) are shown by the dotted, dot-dashed, and dashed curves respectively, while the hatched region gives the combined constraint. The indirect measurement from the global CKM fit is shown with its error bar.

This direct measurement of α is in good agreement with the indirect measurement from the global CKM fit. Direct measurements of α based on SU(3) symmetry in the $B \to \rho\rho$ modes and in the $B \to a_1\pi$ modes give also compatible results. The precision on α has improved with the new result from *BABAR* on the $B^+ \to \rho^+\rho^0$ branching fraction. It is now less than 5%, a precision which seemed out of reach at the start of the B factories.

References

[1] N. Cabibbo, Phys. Rev. Lett. 10, 531 (1963); M. Kobayashi and T. Maskawa, Prog. Theor. Phys. 49, 652 (1973).

[2] *BABAR* Collaboration, B. Aubert *et al.*, Nucl. Inst. and Meth. A 479, 1 (2002); Belle Collaboration, A. Abashian *et al.*, Nucl. Inst. and Meth. A 479, 117 (2002).

[3] M. Gronau and D. London, Phys. Rev. Lett. 65, 3381 (1990).

[4] Belle Collaboration, H. Ishino *et al.*, Phys. Rev. Lett. 98, 211801 (2007).

[5] *BABAR* Collaboration, B. Aubert *et al.*, arXiv: 0807.4226 (2008).

[6] *BABAR* Collaboration, B. Aubert *et al.*, Phys. Rev. D 76, 091102 (2007).

[7] *BABAR* Collaboration, B. Aubert *et al.*, Phys. Rev. D 75, 012008 (2007).

[8] Belle Collaboration, K. Abe *et al.*, hep-ex/ 0610065 (2006).

[9] Belle Collaboration, S.-W. Lin *et al.*, Nature 452, 332 (2008).

[10] Belle Collaboration, S.-W. Lin *et al.*, Phys. Rev. Lett. 99, 121601 (2007).

[11] Heavy Flavor Averaging Group (HFAG), http://www.slac.stanford.edu/xorg/hfag.

[12] Belle Collaboration, A. Somov *et al.*, Phys. Rev. D 76, 011104 (2007).

[13] *BABAR* Collaboration, B. Aubert *et al.*, Phys. Rev. D 76, 052007 (2007).

[14] *BABAR* Collaboration, B. Aubert *et al.*, Phys. Rev. D 78, 071104 (2008).

[15] *BABAR* Collaboration, B. Aubert *et al.*, Phys. Rev. Lett. 102, 141802 (2009).

[16] Belle Collaboration, A. Somov *et al.*, Phys. Rev. Lett. 96, 171801 (2006).

[17] Belle Collaboration, J. Zhang *et al.*, Phys. Rev. Lett. 91, 221801 (2003).

[18] Belle Collaboration, C.-C. Chiang *et al.*, Phys. Rev. D 78, 111102 (2008).

[19] M. Beneke *et al.*, Phys. Lett. B 638, 68 (2006).

[20] Belle Collaboration, J. Zhang *et al.*, Phys. Rev. Lett. 95, 141801 (2005).

[21] *BABAR* Collaboration, B. Aubert *et al.*, Phys. Rev. Lett. 97, 201801 (2007).

[22] A. Snyder and H. Quinn, Phys. Rev. D 48, 2139 (1993).

[23] *BABAR* Collaboration, B. Aubert *et al.*, Phys. Rev. D 76, 012004 (2007).

[24] Belle Collaboration, A. Kusaka *et al.*, Phys. Rev. D 77, 072001 (2008).

[25] *BABAR* Collaboration, B. Aubert *et al.*, Phys. Rev. Lett. 97, 051802 (2006).

[26] Belle Collaboration, K. Abe *et al.*, arXiv: 0706.3279 (2007).

[27] *BABAR* Collaboration, B. Aubert *et al.*, Phys. Rev. Lett. 98, 181803 (2007).

[28] M. Gronau and J. Zupan, Phys. Rev. D 73, 057502 (2006).

[29] *BABAR* Collaboration, B. Aubert *et al.*, Phys. Rev. Lett. 100, 051803 (2008).

[30] *BABAR* Collaboration, B. Aubert *et al.*, arXiv: 0909.2171 (2009).

[31] CKMfitter group, Eur. Phys. J. C41, 1 (2005), updated at http://ckmfitter.in2p3.fr.